An innovative material for space-oriented structures and habitat design

Giacomo Frulla and Enrico Cestino
DIMEAS, Politecnico di Torino, Turin, Italy
Federico Cumino
Aerospace Consultant, Torino, Italy
Alessio Piccolo
DIMA, Facoltà di Ingegneria, Università degli Studi di Roma La Sapienza, Roma, Italy
Nicola Giulietti and Eugenio Fossat
Composite Research s.r.l. (Co.Re), Torino, Italy, and
Ehsan Kharrazi
Aerospace Consultant, Torino, Italy

Abstract

Purpose – The purpose of this study is to investigate a new and innovative sandwich material evaluating its capability for use in space habitat structural components in deployable and foldable configurations. The main habitat requirements were considered in the preliminary design of a typical space outpost, proposing a preliminary architecture.

Design/methodology/approach – The stiffness properties of the innovative sandwich (MAdFlex ®) were evaluated using numerical and experimental investigations. Four-point bending tests were performed for complete sandwich characterization. Numerical FE simulations were performed using typical material properties and performance. The application to a space habitat main structure as a basic material has also been discussed and presented.

Findings – MAdFlex basic stiffness performances have been determined considering its double behavior: sufficiently stiff if loaded in a specific direction, flexible if loaded in the opposite direction and enhanced folding performance. Successful application to a typical space habitat confirms the validity and convenience of such a material in designing alternative structures.

Research limitations/implications – The innovative material demonstrates wide potential for structural application and design in demanding space situations under operating conditions and in stored ones at launch.

Practical implications – Several simple deployable structural components can be designed and optimized both for the space environment and for the more traditional terrestrial applications.

Social implications – Simplification in structural design can be derived from deployable low-weight items.

Originality/value – Innovative customized material in sandwich configuration has been proposed and investigated with the aim to demonstrate its potentiality and validity in alternative design architecture.

Keywords Innovative sandwich configuration, Stiffness properties, Habitat design and space applications

Paper type Research paper

Introduction

The concept of space as an inaccessible place, except for a few people, is rapidly changing, and the idea of commercial travel and space tourism are coming with their positive and negative aspects. The mission cost and the harsh space environment are the greatest obstacles to cope with, however, a lightweight and deployable habitat could be the first step making this new era of space exploration a possible opportunity. Before and after the first landing on the Moon on July 20, 1969, many engineers and architects developed and designed habitats with the most different characteristics, materials and shapes to better achieve the main goal: design a safe and comfortable place where a man can live for a certain period. However, most of these ideas were

The current issue and full text archive of this journal is available on Emerald Insight at: **https://www.emerald.com/insight/1748-8842.htm**

Aircraft Engineering and Aerospace Technology
95/11 (2023) 14–24
Emerald Publishing Limited [ISSN 1748-8842]
[DOI 10.1108/AEAT-06-2022-0170]

The experimental activity presented in this paper has been developed with the support of Co.Re S.r.L.

Received 12 July 2022
Revised 14 October 2022
Accepted 28 October 2022

developed through purely architectural consideration, without extensive structural, thermal and other specific types of analyses. Numerous types of habitats have been presented in the literature for future Lunar and Martian settlements. Some of the most interesting and innovative solutions can be summarized in the following, highlighting the most ingenious and peculiar features.

The first considered habitat design was proposed by Boeing in 1963: LESA (Lunar Exploration System for Apollo). It was a rigid module designed to accommodate six people for six months with 46,000 lb of payload, a 10 kW nuclear reactor, a 3,765 lb rover and equipment to move regolith for shielding as Benaroya (2018), Adams (1998). Kaplicky and Nixon (1985) developed a moon base concept able to accommodate six astronauts with six rigid modules with a length of 10 m and a diameter of 4.5 m. This research outpost including housing, logistic and laboratory modules, simply and manually deployable superstructure was covered by regolith for shielding (as Ganapathi *et al.*, 1993). A three-hinged arch shell structure was analyzed by Ruess *et al* (2006). A circular configuration was considered more suitable for gravitational loads and internal pressure applying favorable bending moments distribution.

Spheric inflatable lunar habitat was developed in Roberts (1988), Choen *et al.* (2009), Netti (2019) for the Lunar Base Systems using high-strength aramid fibers for the main structural components providing a 16 m sphere diameter with an internal inflated volume of 2,145 m^3 comfortable for 12 astronauts and their related equipment but packaged to 40 m^3 (packaging ratio of 10:1) when folded before launch. The estimated total mass was of about 16,300 kg including 9,000 kg of primary structures, 6,000 kg of floors and 1,300 kg of walls. A regolith 3 m shield was expected.

Considering the structural design, a tentative classification indicates: rigid structure, inflatable and deployable structure, *in-situ* resources utilization (ISRU)-based structures.

Rigid structures, designed to preserve their shape avoiding high deformation and displacement, include trusses and frame assembly and are usually made by metal or composite material. Until today they represent the most widely used structures in the aerospace field because of high reliability-related materials and high puncture resistance without secondary added elements. Higher mass and fixed volume penalize them in the transport phase.

Terms "inflatable" and "deployable" do not have a standard use in the literature, preferably "inflatable" for soft and foldable materials that are balloon-like, and "deployable" for rigid but storable components that are mostly mechanisms as in Häuplik-Meusburger *et al.* (2009) and Häuplik-Meusburger and Özdemir (2012), Hijazi (1988), Sokolowski and Tan (2007), Vincent (2013). Inflatables are designed using fabrics or membranes including external primary structural elements and internal components made by aluminum or composite. Pressure inside inflatables is a fundamental component in maintaining their operative shape under loads and limited volume obtained in folded configuration at launch is of great interest for space missions (high packaging factor in folded shape, low cost, inflation more than one time). However, they are not commonly used due to low reliability level of the used materials and for low punctual resistance with high bending stress during folding/deploying such as in Benaroya (2018). Examples of inflatable: "Echo 1 balloon", NASA TransHab (1990's) referred by Kennedy (2002, 1999), Bigelow Expandable Activity Module experimental inflatable module for the International Space Station tested in 2016 as Valle and Wells (2017), Seedhouse (2015).

ISRU refers to specific configuration based on the material and resources found in the settlement area for reducing the mission costs due to material and/or components transportation. External structures, made by local material, are manufactured for protecting the habitat from high temperature variation during local day, ionizing radiation impacting in material degradation and astronauts' health and so on. Useful *in-situ* resource is the regolith: a blanket of unconsolidated, loose, heterogeneous superficial deposits covering solid rock. It includes dust, broken rocks and other related materials present on Earth, Moon, Mars, some asteroids and other terrestrial planets and moons as described by Meyer (2003). The regolith can be used as structural material if combined with water (but increasing mission costs if transported from Earth) or sintered using casting procedure or 3D printing as in Ruess *et al.* (2006).

A lightweight and deployable habitat design has been proposed in the following sections as a possible application of an innovative material ensuring long-duration missions on the lunar/planet surface. A new innovative sandwich configuration (MAdFlex ®) has been proposed by Composite Research S.r.L. Co. Re (2020) to cope with requirement of good strength and foldable properties as requested by this type of structural system and alternative application as in Gili and Frulla (2016). The MAdFlex has been designed to be crushproof if loaded on one side and flexible, even rollable, if loaded on the other side by means of selecting the right material for sandwich faces. This combination has been demonstrated to be very attractive in deployable habitat design. Main design requirements have been identified and collected together with the characterization of the stiffness properties of selected innovative material directly applied to the proposed habitat architecture.

General requirements and preliminary habitat configuration

Requirements definition is a fundamental step in every design procedure. Several items have been selected and summarized here to provide an initial step in the preliminary design procedure with respect to architectural, internal environment, structural and launcher needs. Architectural requirements usually refer to those factors influencing the volume and form of the habitat. The physical and psychological needs of humans in a confined environment must be balanced against the physical limitations of a pneumatic structure as described by Vincent (2013). These factors can be summarized as follows: habitable volume per person excluding volume occupied by equipment and other items, height of the habitat, total floor area per person.

Gemini missions provided about 0.57 m^3 available volume per crew member for a short-duration mission while a volume of about 20 m^3 per crew member was extrapolated by Rudsill (2008), Ruess (2006) and NASA (1995) for a duration longer than 5 months to guarantee the optimal performance level. A free volume per crew member of 120 m^3 including living and working areas can be considered as a free space requirement. This value is comparable to the actual available volume per astronaut on the ISS. Proposed heights range from 2.44 m to 4.0 m as in Kennedy (1999). The available floor per person is about 40 m^2 based on a free volume of 120 m^3 per crew member and an effective available height of 3 m. Multiplying this latter value for the number of crew members a preliminary estimation of the total floor area is provided and the required number of modules determined.

Preliminary habitat shape definition can be assessed assuming a deployable configuration. The external and internal geometry of the module coupled with the material chosen for the primary structure allows the folding and deploying process with the ability to withstand the regolith cover and minimize the structural mass. Extensive MAdFLex application as in Cumino *et al.* (2021) empirically demonstrated two more convenient configurations for deployable habitats: cylinder ad dome. Deployable process expected for cylinder and dome as Cumino *et al.* (2021) has been reported in Appendix A-1 as an example. A necessary shielding architecture has to be determined to maintain a consistent internal environment related to mission needs. Guidelines released by National Council on Radiological Protection and Measurements and reported in Sinclair (1981) can be established for a specific shield definition: common material used for shielding is the regolith positioned outside the habitat. Different combinations of regolith and regolith mixed with available liquid can be evaluated. The internal pressure of about 1 atm (such as in ISS), based on a dual-gas atmosphere (oxygen-nitrogen) has been considered Cohen and Benaroya (2009). Other fundamental environmental requirements are defined as in Chen *et al.* (2020) and Chen *et al.* (2021) but not included into the presented investigation.

The structural design required the selection of a representative safety factor (SF) as one of the most important items in the design. Aerospace SF on Earth ranges approximately from 1.7 to 3.5 for commercial applications. According to Ruess (2006), a factor of safety of about 4 or higher seems reasonable in preliminary design activity for non-Earth structural construction due to *in-situ* material related uncertainty. The identification of the main design load conditions is again of primary importance to achieve the right structural sizing of the selected configuration. The main ones are reported in the following:

- internal pressure of 1 atm ($1{:}013 * 10^5$ Pa) only;
- internal pressure of 1 atm ($1{:}013 * 10^5$ Pa), plus regolith cover load (regolith thickness: 2.5 m minimum);
- regolith cover load only (regolith thickness: 1.65 m – regolith type W50 water mixture with adesite rock as in Piccolo, 2021 and Sasa 2020); and
- load used to keep the habitat in the folded configuration at launch or storage phase.

Conditions n.1 and n.2 are obvious if a correct deployment and installation has been determined. Condition n.3 represents an "emergency-state" when the pressure has been lost or planned de-pressurization for a specific operation has been established: collapse and crushing persons inside has to be avoided. Condition n.4 is related to preparing the payload at lunch or deploying it at arrival. The structure must withstand these main load conditions both considering strength and stiffness criteria including preliminary stability problems. Payload needs are connected to the launcher and fairing dimensions. As an example the SLS block 1B cargo & 2: 19,1 m (62.7 ft) in height and an internal diameter (value of interest) of 7,5 m(24.6 ft) with usable volume of about 229.9 m^3 (8118 ft^3). The maximum transportable mass depends on the available trust and the mission target. As an example the same SLS block 1B cargo & 2 has a maximum payload mass of about 42t (92.5k lbs).

A dome shape configuration (internal radius about 3.5 m with regolith covering thickness according to the selected shielding ability and 1 atm internal pressure) can be considered in the following sections as a design candidate for the application of innovative MAdFlex performance.

Innovative material characterization and properties

The innovative MAdFlex material created by Composite Research (Co.Re.) is a sandwich-like structure with dual-stiffness properties when loaded along one side or along the opposite side with interesting folding properties as pointed out in Figure 1. Rigid skin (n.1 in Figure 1) is commonly made by carbon, glass or aramid laminates while Dyneema high density polyethylene fibers is used for the flexible one as in Kharrazi (2020), Cumino (2020), Piccolo (2021) Co.Re. (2020). Compared to the conventional aluminum scheme a similar stiffness response is demonstrated but with a weight saving of about four times. Details and analytical evaluation are summarized in Table 1 as specified in Appendix A1-2 for the analytical evaluation. The specimens are 300 mm long, 21 mm wide, and 5.48 mm thick with and without grooves in the core. The loading and restraint conditions are the same for both cases (simply supporting distance of 200 mm). Two series of loads are placed on the upper skin when rigid configuration is considered while mirroring the load has been done for the flexible case simulation. A total of 25 nodes are considered in *y*-direction for a total load of about 100 N and 20 N for the rigid and flexible case, respectively. As far as the flexible side is concerned, a maximum load of about 5 N has been applied due to different local phenomena arising at higher load level.

Figure 1 MadFlex section view in foldable configuration

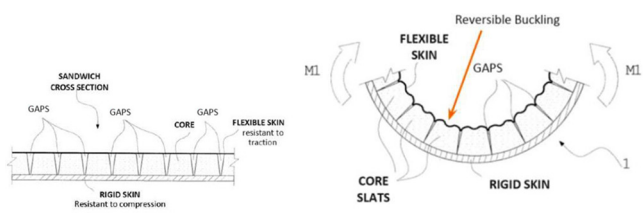

Note: (Co. Re, 2020)

Table 1 Dimensions and properties for preliminary analytical calculation

B (mm)	21	Gc (Mpa)	30	GA* (N)	3459,6	S;L (mm)	200;40
T1 (mm)	0.24	E1(E1-weak)(Mpa)	11,000 (300)	E-A (N)	55008,6	P (N)	100
Tc (mm)	5	Ec (Mpa)	60	E-B (Nmm)	−293153,6	v-max (stiff-side) (mm)	12.63
T2 (mm)	0.24	E2 (Mpa)	77100	E-D (Nmm^2)	1,371,444	v-max(weak-side) mm)	31.6

A Numerical FE (commercial PATRAN/NASTRAN software) model has been prepared to investigate the MAdFlex preliminary stiffness behavior and compare it with an analytical/experimental one. Specific nonlinear phenomena connected to MAdFlex configuration at high loads requiring detailed nonlinear investigation, will be postponed to future analyses and are outside the scope of the actual discussion. The flexible layer is described as an "equivalent quasi-isotropic" material 0.24 mm thick with non-linear characteristics (bi-modulus) as reported in Appendix A-2, while the rigid skin is instead made by a carbon fiber laminate [0°/90°] 0.24 mm thick with similar tension-compression performance (see Appendix A-2 for details).

Finally, the core foam is modeled as an "equivalent isotropic" elastic material with a total thickness of 5 mm and a particular geometry as in Appendix A-2. The loading and boundary condition scheme is specified in Appendix A-1, referring to the "fourth point bending test" according to ASTM D7250/D7250M (2011) as reported in Appendix A1. A 2D finite element modeling has been considered for the thin faces while 3D elements have been considered for the core. Numerical non-linear analysis has been performed by means of SOL400 NASTRAN implicit method with load increment of 5% at a time. The "core-without-groove" configuration is analyzed at the beginning in order to compare it with the analytical simplified derivation and validate the procedure (Appendix A-1). A maximum deflection of 14.2 mm and 30.5 mm for the rigid and flexible cases respectively. Analytical related procedure indicates a maximum deflection of 12.63 mm and 31.6 mm for the two conditions with a relative error of about 11% and 3%, respectively. The validity of the analytical proposed procedure for MAdflex stiffness evaluation has been demonstrated, and it is considered acceptable for preliminary design purposes.

The "core-with-groove" configuration is evaluated in a second phase by numerical/experimental comparison. Three bending tests are available both for the rigid configuration and for the flexible one. Higher deflections are determined due to the change in core configuration. No analytical simulation has been provided for this case due to specific nonlinear expected behavior that is out of the scope of the present investigation. Numerical results show a maximum deflection of 14.9 mm (rigid configuration) under a load of 100 N and a maximum deflection of 42.5 mm (flexible one) subjected to a maximum load of 20 N. The rigid case experimental/numerical comparison is reported in Figure 2(a) for three specimens, A,B,C, conventionally indicated as DB220A, DB220B, DB220C arranged with the same configuration as previously described and loaded along rigid behavior . Stiffness is almost well behaved so confirming the validity of the procedure. The compressed carbon skin exhibits a maximum stress of about 262 MPa while the equivalent-Dyneema tensile is about 151 MPa. The numerical simulation has been limited to the first part of the loading curve leaving the investigation of the subsequent nonlinear behavior for future research activities. Figure 2(b) presents numerical/experimental comparison for the flexible configuration related to four specimens, Ab1, Ab2, Ab10, Cb10 with the same configuration as previously reported but loaded along the flexible side and conventionally indicated as DB220Ab1 and DB220Ab2 (bent twice), DB220Ab10 (bent ten times), DB220Cb10 (bent ten times). Neglecting variation in mechanical properties of the single MAdFlex component after few bends, a certain difference in sample static behavior is reported in Figure 2(b) that shows almost the same initial stiffness for all the samples, but different behavior at higher loads more pronounced for the Ab10 and Cb10 ones but evident also for the case of bent twice. An effect of preliminary bent configuration has been determined. Similar considerations as for the rigid case, can be done referring to the second part of the experimental plot. A good correspondence has been determined also in this case encouraging the presented research activity to proceed toward a more detailed investigation for high order phenomena related to such a material situation as: Local buckling of Dyneema in the groove position and a groove-walls contact problem under high load (Appendix A-2). Carbon skin in tension exhibits a maximum tensile stress of approximately 83 MPa while

Figure 2 Load vs max displacement curve (FEM and experimental with grooves)

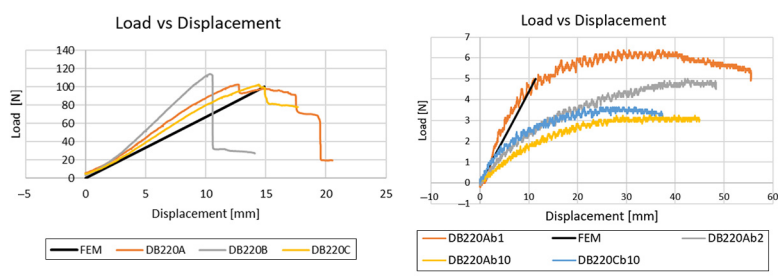

(a) (b)

Notes: (a) Rigid configuration; (b) flexible configuration

the equivalent Dyneema is compressed at a stress level of about 12 MPa.

Proposed configuration for Lunar and Martian habitat

Previously defined sandwich scheme has been considered as reference material for evaluating extra-terrestrial habitat architecture. The potentiality of such a configuration has been emphasized as the key-point in successful design of such a demanding idea. Potential exploitable capability has been investigated as related to different mission of the same rank as in Cumino *et al.* (2021). Volume, internal pressure and external shield of regolith weighting and covering the internal area, are considered as basic requirements in design procedure. FE simulation has been performed for a realistic performance evaluation of the assumed structure. According to the initial design requirements, previously presented, both the case of external regolith shield and the inclusion of internal pressure are numerically evaluated and discussed. The selected configuration has to withstand the covering regolith shield also in emergency/failure situations of no internal pressure. An internal pressure of about 1 atm added to the external regolith load is assumed in "normal" operating conditions. The proposed cylindrical architecture or dome-shape architecture has been manufactured following a similar modular concept: a combination of internal structural arches connected by flexible envelope. Extensive application of MAdFlex material is considered for the arches due to its specific properties (strength and folding capability) as previously presented. Flexible layered Dyneema or specific MAdFlex material can be instead introduced for the connecting envelope. The Dome-shape module design is selected as representative study case. It is composed by eight arch-branches made by MAdFlex sandwich structural elements, interspersed with an envelope made by layered Dyneema. The arches are connected by hinges with the floor and the connecting upper plate in order to facilitate its folding characteristics. The structural scheme and loading conditions are presented in Figure A13 in Appendix 2 with specific configuration details.

Figure 3(a) and (b) show dome-shape displacements under emergency and operating conditions. Regolith load acts alone in emergency case with maximum displacements of about 153 mm in the envelope. The top-connecting plate shows a slight lowering of 48 mm leaving a good margin for people inside if compared to the 3500 mm height. Stress distribution provides following results: Carbon fiber (CFRP) composite skin stress values range from −32 to 15 MPa and from −9 to 28 MPa for Dyneema. The stresses in the core, for the half-arches, go from −0.1 MPa to 0.12 MPa. The equivalent Dyneema envelope layer is entirely in traction reaching a maximum stress of 104 MPa. A displacement of 0.127 mm upwards for the top of the structure is solved out in operating condition, while the equivalent Dyneema envelope layer has a displacement of 14 mm outwards. The stress values in the CFRP skin range from −134 to 102 MPa, from −40 to 188 MPa for Dyneema skin and from −0.73 MPa to 0.86 MPa for the core (variable also in function of the thickness and depending to the connected face). These results demonstrated that the internal pressure manages to win over the load of the external regolith, tending to make the structure swell. Considering the novelty content in such a design and the typical related mission (be capable to resist a journey to Mars, land on the surface and protect the astronauts for the entire duration of the permanence *in situ* while resisting the regolith and the internal pressure), a SF of 4 is considered. Ultimate stress have been compared to the

Figure 3 MadFlex dome results

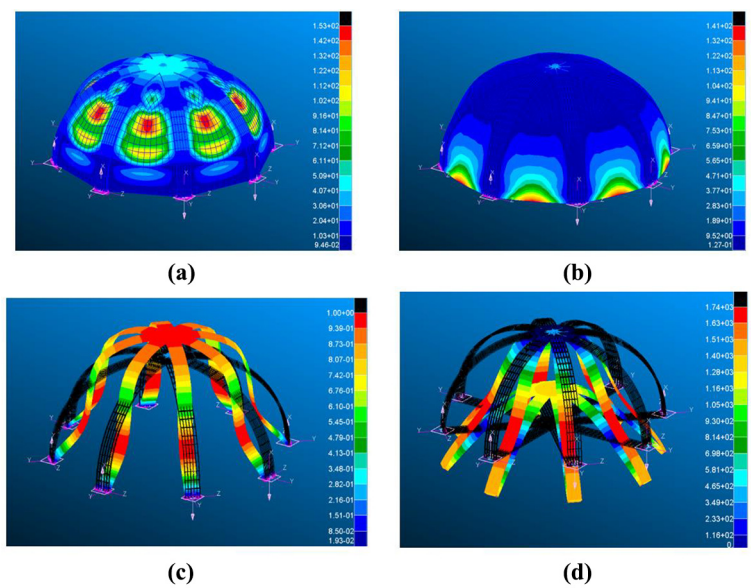

Notes: (a) Displacements with only regolith load; (b) displacements with regolith and internal pressure load; (c) First buckling shape; (d) folded configuration. (Piccolo, 2021)

maximum stress of the materials as reported in Table A2 demonstrating the strength validation of such a configuration. Evaluation of critical condition under loads and wrinkling phenomenon completes this preliminary design step. Face wrinkling for the carbon skin provides a stress value of about 490 Mpa that is lower than the applied compressive load. Typical global buckling load factor according to SOL105 has been solved out of about 1.22 with a buckling shape according to Figure 3(c): no buckling condition within the operating load envelope has been demonstrated (Piccolo, 2021). Folding properties and folded shape have been determined. The possibility of reducing its volume is given by the fact that the semi-arches of the dome are connected to the floor elements by means of hinges and the right positioning of the Dyneema skin in MAdFlex enhance the folding curvature of arches. The closure procedure takes place by bringing the floor inward and the semi-arches almost touching each other without failure situation. Figure 3(d) reports a step in the folding operation: the radius of the closed structure is about half the radius of the expanded structure, leading to a significant decrease in required volume than can be easily stored inside the cargo-bay at launch. A weight of about 570 kg has been determined demonstrating its consistency to the requirement at launch for a typical launcher such as SLS block 1B. Feasibility of the proposed configuration is so demonstrated.

Conclusion

A preliminary evaluation of innovative material for habitat design has been performed. Stiffness characteristics are worked out and pointed out for specific definition of main structural elements in space habitat definition. The preliminary habitat configuration has been designed including preliminary structural simulation to take into consideration main design requirements for such a space application. Operating and emergency situations have been considered as design constraint demonstrating the feasibility of the proposed habitat and feasibility of the material application. The selected configuration has been demonstrated to cope with the design requirements revealing a maximum dome deflection lower than 155 mm under critical operative condition without reaching a critical shape situation. It also demonstrates to be consistent to the weight requirement of about 570 kg as referred to actual launcher SLS data. The folding properties are also considered in the simulation as a basic item in the proposed design. Folding procedure and related residual volume are evaluated for a comparison to available space in commercial launch cargo bay. The proposed architecture demonstrates consistency to the requirements also if an optimization activity could improve the selected sizing. The proposed innovative material can be considered as one of the main candidates to be selected for space habitat design and space mission.

References

Adams, C.M. (1998), "Defin(design)ing the human domain: the process of architectural integration of long-duration space facilities", SAE Technical Paper 981789. Warrendale, PA.1998. International Conference On Environmental Systems. ISSN: 0148-7191.e-ISSN: 2688-3627. Also in: SAE 1998 Transactions - Journal of Aerospace-V107-1.

ASTM D7250/D7250M (2011), "Standard practice for determining sandwich beam flexural and shear stiffness", ASTM International 2011.

Benaroya, H. (2018), "Lunar habitats: a brief overview of issues and concepts", *REACH*, Vols 7/8.

Chen, M., Goyal, R., Majji, M. and Skelton, R.E. (2020), "Design and analysis of a growable artificial gravity space habitat", *Aerospace Science and Technology*, Vol. 106, p. 106147.

Chen, M., Goyal, R., Majji, M. and Skelton, R.E. (2021), "Review of space habitat designs for long term space explorations", *Progress in Aerospace Sciences*, Vol. 122, p. 100692.

Co. Re (2020), *Madflex Sample Book*, Composite Research, Torino.

Cohen, M.M. and Benaroya, H. (2009), "Lunar-base structures", in Scott Howe, A. and Brent S. (Eds), *Out of This World, the New Field of Space Architecture*, Copyright © 2009 by the American Institute of Aeronautics and Astronautics. pp. 179-204, doi: 10.2514/5.9781563479878.0179.0204. Published online August 2012, doi: 10.2514/4.479878.

Cumino, F. (2020), "Preliminary design of deployable habitat for lunar outpost made by innovative material", Final Thesis. Polytechnic of Turin.

Cumino, F., Frulla, G., Cestino, E., Fossat, E., Giulietti, N. and Piccolo, A. (2021), "Deployable habitat for a future lunar outpost", Composite Magazine. Vol. anno XVI (n.59), 2021, pp.4-9. ISSN:2499-6890. Ed. Milano: Tecnedit Vimercate (MI): SEM.

Ganapathi, G.B., Ferrall, J. and Seshan, P.K. (1993), "Lunar base habitat designs: characterizing the environment, and selecting habitat designs for future trade-offs", NASA-CR-195687, JPL Publication 93-20. 1993.

Gili, P. and Frulla, G. (2016), "A variable twist blade concept for more effective wind generation: design and realization", *Smart Science*, Vol. 4 No. 2, pp. 78-86, doi: 10.1080/23080477.2016.1191002, ISSN:2308-0477.

Häuplik-Meusburger, S. and Özdemir, K. (2012), "Deployable lunar habitation design", *Book: Prospective Energy and Material Resources*, 1st ed., Chapter 20, Springer-Verlag New York, LLC, New York, NY, pp. 469-502.

Häuplik-Meusburger, S., Sommer, B. and Aguzzi, M. (2009), "Inflatable technologies: adaptability from dream to reality", *Acta Astronautica*, Vol. 65 Nos 5/6, pp. 841-852, doi: 10.1016/j.actaastro.2009.03.036.

Hijazi, Y. (1988), "Prefabricated foldable lunar base modular systems for habitats, offices, and laboratories", *2nd Conference on Lunar Bases and Space Activities. In NASA Conf. Publ. 3166, NASA, Washington, DC*, 1992.

Kaplicky, J. and Nixon, D. (1985), "A surface-assembled superstructure envelope system to support regolith mass-shielding for an initial-operational-capability lunar base", in Mendell, W.W. (Ed.), *Lunar Bases and Space Activities of the 21st Century. Lunar and Planetary Institute, Houston*, p. 375.

Kennedy, K.J. (1999), "ISS TransHab architecture description", *Proceedings of the 29th International Conference on Environmental Science (ICES); Society of Automotive Engineers, Warrenburg, PA*.

Kennedy, K. (2002), "Lessons from TransHab: an architect's experience", *AIAA Space Architecture Symposium*, 10-11 October 2002, *Houston, TX*, AIAA 2002-6105.

Kharrazi, E. (2020), "Structural FEM analysis of innovative sandwich configuration for automotive application", Final Thesis, Politecnico di Torino, TO.

Meyer, C. (2003), "The lunar petrographic", Educational Thin Section Set. Astromaterials Curation NASA Lyndon B. Johnson Space Center Houston, Texas 77058. September 2003.

NASA (1995), "NASA-STD-3000, volume I – man-systems integration standards, architecture, envelope geometry for crew functions", Revision B. 1995.

Netti, V. (2019), "DMF: deployable modular frame for inflatable space habitats", IAC-19,B3,8-GTS.2,4,x48931, *70th International Astronautical Congress (IAC)*, *Washington, DC*, 21-25 October 2019, Copyright ©2019 by the International Astronautical Federation (IAF).

Piccolo, A. (2021), "Preliminary design of deployable martian habitat made by innovative material", Final Thesis, Politecnico di Torino, TO.

Roberts, M. (1988), "Inflatable habitation for the lunar base", in Mendell, W.W. (Ed.), *The Second Conference on Lunar Bases and Space Activities of the 21st Century, Proceedings*, *Houston, TX*, April 5-7, 1988, NASA Conference Publication 3166, 1992, *NASA Johnson Space Center*, p. 249.

Rudsill, M., Howard, R., Griffin, B., Green, J., Toups, L. and Kennedy, K. (2008), "Lunar architecture team: phase 2 habitat volume estimation: caution when using analogs", Researchgate September 2008, doi: 10.1061/40988(323)10.

Ruess, F., Schaenzlin, J. and Benaroya, H. (2006), "Structural design of a lunar habitat", *Journal of Aerospace Engineering*, Vol. 19 No. 3, pp. 133-157, 2006. ©ASCE, ISSN 0893-1321/2006/3-133–157/$25.00, doi: 10.1061/ASCE0893-1321200619:3133.

Seedhouse, E. (2015), "Bigelow expandable activity module", *Bigelow Aerospace*, Springer International Publishing, Switzerland, pp. 87-98, doi: 10.1007/978-3-319-05197-0.

Sokolowski, W.M. and Tan, S.C. (2007), "Advanced self deployable structures for space applications", *Journal of Spacecraft and Rockets*, Vol. 44 No. 4, pp. 750-754, Jul. 2007, ISSN: 00224650, doi: 10.2514/1.22854.

Valle, G. and Wells, N. (2017), "Bigelow expandable activity module (BEAM) ISS Year-One", *BEAM Project Management and Instrumentation Team ISS R&D Conference*, *Washington, DC*, 19-July-2017.

Vincent, R., Vrakking, J.G. and Shubert, D. (2013), "Design of a deployable structure for a lunar greenhouse module", *AIAA 2013-3352. 43rd International Conference on Environmental Systems*, July 14-18, 2013, *Vail, CO*. Session: Thermal and Environmental Control of Exploration Vehicles and Surface Transport Systems. Published Online:11 July 2013, doi: 10.2514/6.2013-3352.

Further reading

Röstel, L., Guo, J., Banjac, S., Wimmer-Schweingruber, R.F. and Heber, B. (2020), "Subsurface radiation environment of mars and its implication for shielding protection of future habitats", *Journal of Geophysical Research: Planets*, Vol. 125 No. 3.

Appendix 1

Example of deployable configuration

The following Figures (A1, A2, A3 and A4) show deployable process expected for cylinder and dome as Cumino *et al.* (2021).

Figure A1 Cylinder deployed rendering global view

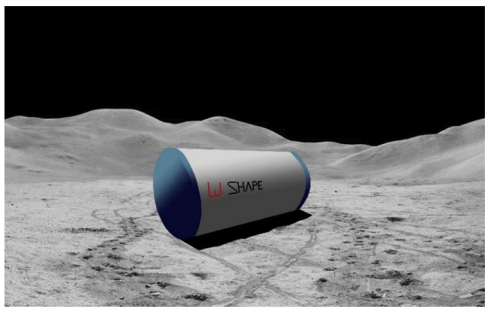

Figure A2 Deployable sequence for cylinder configuration

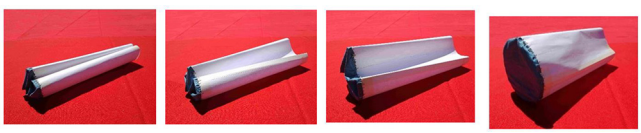

Figure A3 Dome deployed rendering view – closed configuration

Figure A4 Possible dome deployable sequence as an example – upper plate moving outward tensioning cables and opening envelope

Innovative sandwich analytical simulation

The hybrid sandwich beam analytical evaluation is based on the well-known sandwich theory and assumptions considering different materials and thickness. The innovative MadFlex material created by Composite Research (Co.Re.) is a sandwich-like structure with dual-stiffness properties when loaded along one side or along the opposite side. The "comp" face in Figure A5 is able to withstand tension/compression load, while the "dyn" face is characterized by stiff properties in tension and very low stiffness in compression. The whole section contributes to the bending stiffness when rigid skin is in compression and the flexible one in traction. On the contrary if the flexible skin is under compression it does not contribute to the sandwich stiffness and consequently the sandwich folds, under very low load level

The E1, Ec, E2 are the representative modulus of the "dyn" layer, core and "comp" layer, respectively, for the sandwich beam. The base b is the width of the sandwich beam, while t1, tc, t2 are the relative thickness of the sandwich components. Sandwich constitutive equations (Pz, Mx relative axial load and bending moment, respectively, on the sandwich beam connected to axial strain and bending curvature) and equivalent related stiffness (A^*, B^*, D^* extensional, coupling and bending respectively) are reported in equation A1-1 with centroidal calculated position Yc. Equation A1-2 reports the inverse relation among the same variables.

$$\begin{Bmatrix} P_z \\ M_x \end{Bmatrix} = \begin{bmatrix} A^* & B^* \\ B^* & D^* \end{bmatrix} \begin{Bmatrix} \varepsilon_z \\ \theta_{,z} \end{Bmatrix}$$

$$\begin{aligned} A^* &= b\{E_1 t_1 + E_c t_c + E_2 t_2\} \\ B^* &= \frac{b}{2}\left\{E_1 y_1^2 + E_c\left(y_2^2 - y_1^2\right) + E_2\left(y_3^2 - y_2^2\right)\right\} \quad Y_c = \frac{B^*}{A^*} \\ D^* &= \frac{b}{3}\left\{E_1 y_1^3 + E_c\left(y_2^3 - y_1^3\right) + E_2\left(y_3^3 - y_2^3\right)\right\} \end{aligned} \tag{A1-1}$$

$$\begin{Bmatrix} \varepsilon_z \\ \theta_{,z} \end{Bmatrix} = \begin{Bmatrix} \frac{P_z}{E_A} + \frac{M_x}{E_B} \\ \frac{P_z}{E_B} + \frac{M_x}{E_D} \end{Bmatrix} \quad \begin{aligned} E_A &= A^* - \frac{B^* B^*}{D^*} \\ E_B &= \frac{A^* D^*}{B^*} + B^* \\ E_D &= D^* - \frac{B^* B^*}{A^*} \end{aligned} \tag{A1-2}$$

A typical four-points bending arrangement (Figure A6) is considered for stiffness evaluation both analytically and numerically FE determined and compared. ASTM-7520 (2011) has been assumed as representative for test behavior. Equation A1-3 reports the sandwich mid deflection (v-max) and transversal shear stiffness estimates (G-A^*) with G-c the

Figure A5 Sandwich configuration and reference variables

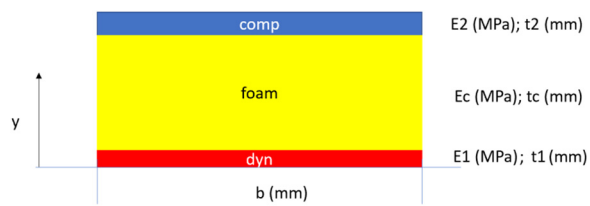

Figure A6 Load and restraint configuration of the sandwich beam according to the standard ASTM D7250/D7250M

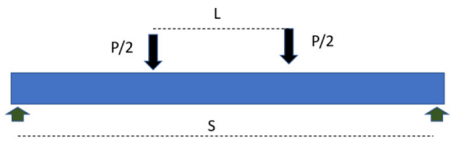

core shear modulus, E-D sandwich bending stiffness, S supporting span, L loading distance, t-I the relative thickness of the sandwich components and P applied load.

$$v_{\max} = \frac{PS^3}{96E_D}\left(2 + \frac{L^3}{S^3} - 3\frac{L^2}{S^2}\right) + \frac{PS}{4G_{A^*}}\left(1 - \frac{L}{S}\right) \qquad \text{(A1-3)}$$

$$G_{A^*} = G_c b \frac{(t_c + 0.5t_1 + 0.5t_2)^2}{t_c}$$

Appendix 2

Numerical simulation details

The mechanical properties introduced in the FEM model are reported in Table A1. Figure A7 presents the bi-modulus characteristic for "equivalent Dyneema" skin while Figure A8 shows the typical core configuration with "groove".

A certain resin penetration inside the foam was observed after cure process (Figure A9) in the interface position with carbon layer. An added layer 0.5 mm thick was introduced inside the FE model [Figure A9(a), and A9(b)] with E = 3000 MPa and G = 1500 MPa as in Kharrazi (2020). Solid and shaped core have been considered in the FE simulation for a better experimental correlation.

The groove simulation has been provided with a mesh densification in the central part of this side, for a better representation of the structural behavior [Figure A9(c)].

Table A1 Material mechanical properties for FEM analysis

Material	$E_{11\ (tract)}$ [MPa]	$E_{11\ (comp)}$ [MPa]	E_{22} [MPa]	G_{12} [MPa]	ν_{12} [MPa]	Density [Kg/m^3]
Unidirectional CFRP	77100	77100	2900	5500	0.3	1790
Rohacell WF 110	60	60	(isotropic)	30	–	110
Equivalent Dyneema	11000	300	(isotropic)	200	0.02	980

Figure A7 Equivalent Dyneema stress–strain curve considered in FEM model

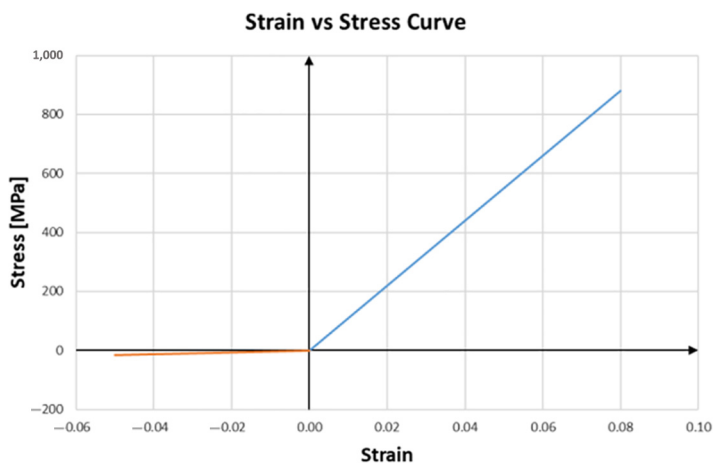

Figure A8 Core geometry in the case of "core-with-grooves"

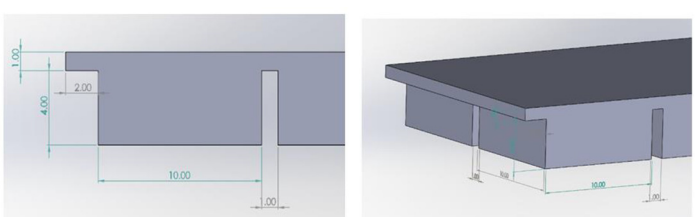

Figure A9 (a) Example of resin penetration inside the foam after Kharrazi, 2020 observation; (b) Modeling of the material composed by resin + foam; (c) Model discretization along *y*-axis

(a) **(b)** **(c)**

Example for numerical deflection results are reported in Figures A10 and A11 in the two indicated sandwich core configuration.

A more detailed investigation has considered necessary for investigating high order phenomena related to such a material situation as in Figure A12. There are two main aspects pointed out by Figure A12: the first is related to the "Local buckling" of Dyneema skin in the groove position

Figure A10 MadFlex without grooves deflections

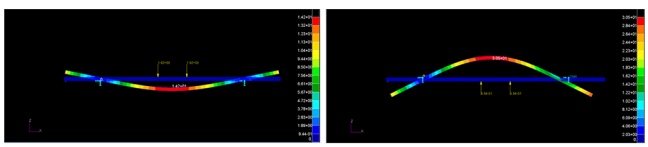

(a) **(b)**

Notes: (a) Rigid configuration; (b) flexible configuration

Figure A11 Max displacement of the rigid configuration with grooves

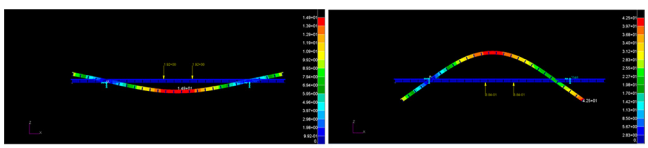

(a) **(b)**

Notes: (a) Rigid configuration; (b) flexible configuration

Figure A12 Equivalent Dyneema local lateral deflection representing local-buckling condition

when it is compressed during a loading situation corresponding to the flexible configuration: a lateral local deflection under load is determined inducing local buckling situation. The limited deformation of the groove walls are due to the small skin stiffness in compression compared to the core stiffness properties in that area. Such a behavior has been considered interesting for further research activity due to the fact that a different numerical approach has to be arranged for a local-global sandwich evaluation. The presented research has been focused on the initial stiffness behavior of such an innovative sandwich configuration. The second aspect is the possible contact along the groove-walls when the load level is enough to reduce the groove gaps to zero. Also this case required a devoted research activity not included in this one.

Proposed habitat scheme for numerical evaluation

The structural scheme and loading configuration are presented in Figure A13. The regolith shield inertial loading condition is considered assuming Mars application with gravitational acceleration of 3.71 m/s^2. The regolith thickness of 1,650 mm with a density of 1,400 kg/m^3 is applied all over the dome and similar loading scheme is derived for the Dyneema envelope 5 mm thick. Main hemisphere arch radius is about 3,500 mm and width of 500 mm, sandwich thickness is as 80 mm for the foam core and 2.8 mm for the skins made by CFRP/ Dyneema. The CFRP skin is placed on the upper part of the MadFlex sandwich (external) while the Dyneema skin is placed in the lower part (inside the dome) fulfilling the required structural strength and the possibility to close the

Figure A13 (a) MadFlex dome internal structure; (b) MadFlex dome internal structure with regolith load; (c) complete multi-arch structure as in Piccolo (2021)

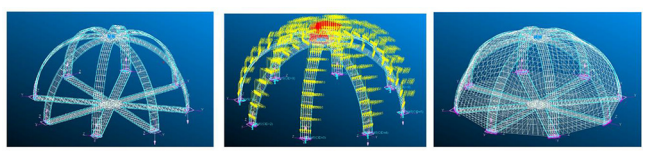

(a) **(b)** **(c)**

Figure A14 Arch loading section with nodal loads for the considered dome configuration

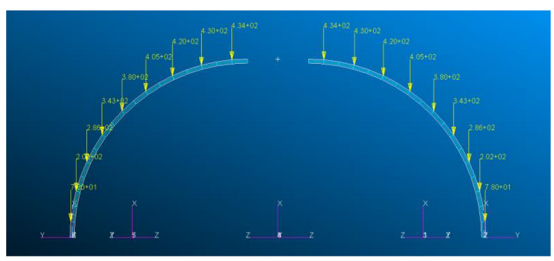

Note: The two semi-arches are connected by an octagonal top-plate as reported in Figure A13 (Piccolo 2021)

Table A2 Material mechanical properties used in MadFlex dome for Mars

Material	$E_{11\ (tract)}$ [MPa]	$E_{11\ (comp)}$ [MPa]	E_{22} [MPa]	G_{12} [MPa]	ν_{12}	Density [Kg/m^3]	$\sigma_{u\ (trac)}$ [MPa]	$\sigma_{u\ (comp)}$ [MPa]
Carbon Fiber fabrics	70,000	70,000	70,000	5,500	0.1	1,790	600	570
Rohacell WF 110	180	180	(isotropic)	70	0.2	110	3.7	3.6
Unidirectional Dyneema	100,000	10	100	200	0.05	980	3,300	–
Equivalent Dyneema	50,000	56	(isotropic)	200	0.01	980	3,300	–

habitat in a folded configuration when a reduced minimal volume is required at launch. The upper connecting plate is also made by the same material. 2D elements for skin and 3D elements for the core with material properties according to Table A2 has been introduced in hybrid FE model. An equivalent isotropic nonlinear material is also carried out for the Dyneema skin as previously explained.

Corresponding author

Giacomo Frulla can be contacted at: giacomo.frulla@polito.it